Näher, H. Schaber, U. Zimmermann, *J. Chem. Phys.* **100**, 2322 (1994).
21. L. S. Bartell, *J. Phys. Chem.* **99**, 1080 (1995).
22. G. Scuseria, *Science* **271**, 942 (1996).
23. D. J. Wales, *Mol. Phys.* **78**, 151 (1993); G. Franke, E. R. Hilf, P. Borrmann, *J. Chem. Phys.* **98**, 3496 (1993).
24. J. P. K. Doye and D. J. Wales, *J. Chem. Phys.* **102**, 9659 (1995); *ibid.*, p. 9673.
25. R. E. Kunz and R. S. Berry, *ibid.* **103**, 1904 (1995).
26. D. J. Wales and R. S. Berry, *Phys. Rev. Lett.* **73**, 2875 (1994); R. M. Lynden-Bell and D. J. Wales, *J. Chem. Phys.* **101**, 1460 (1994); D. J. Wales and J. P. K. Doye, *ibid.* **103**, 3061 (1995).
27. T. L. Hill, *J. Phys. Chem.* **57**, 324 (1953); *J. Chem. Phys.* **23**, 812 (1955).
28. ———, *Thermodynamics of Small Systems: Part I* (Benjamin, New York, 1963).
29. J. D. Honeycutt and H. C. Anderson, *J. Phys. Chem.* **91**, 4950 (1987).
30. R. S. Berry and D. J. Wales, *Phys. Rev. Lett.* **63**, 1156 (1989); D. J. Wales and R. S. Berry, *J. Chem. Phys.* **92**, 4283 (1990).
31. D. Lynden-Bell and R. M. Lynden-Bell, *Mon. Not. R. Astron. Soc.* **181**, 405 (1977); M. Bixon and J. Jortner, *J. Chem. Phys.* **91**, 1631 (1989).
32. P. Labastie and R. L. Whetten, *Phys. Rev. Lett.* **65**, 1567 (1990); H.-P. Cheng, X. Li, R. L. Whetten, R. S. Berry, *Phys. Rev. A* **46**, 791 (1992); S. Weerasinghe and F. G. Amar, *J. Chem. Phys.* **98**, 4967 (1993).
33. R. S. Berry, T. L. Beck, H. L. Davis, J. Jellinek, *Adv. Chem. Phys.* **70**, 75 (1988).
34. R. C. Cohen and R. J. Saykally, *J. Phys. Chem.* **94**, 7991 (1990); N. Pugliano and R. J. Saykally, *J. Chem. Phys.* **96**, 1832 (1992); R. J. Saykally and G. A. Blake, *Science* **259**, 1570 (1993).
35. N. Pugliano and R. J. Saykally, *Science* **257**, 1937 (1992).
36. K. Liu *et al.*, *J. Am. Chem. Soc.* **116**, 3507 (1994).
37. K. Liu *et al.*, *Faraday Discuss. Chem. Soc.* **97**, 35 (1994); S. Suzuki and G. A. Blake, *Chem. Phys. Lett.* **229**, 499 (1994).
38. K. Liu, R. J. Saykally, J. D. Cruzan, *Science* **271**, 929 (1996).
39. H. C. Longuet-Higgins, *Mol. Phys.* **6**, 445 (1963).
40. D. J. Wales, *J. Am. Chem. Soc.* **115**, 11180 (1993).
41. ———, in preparation.
42. J. E. Fowler and H. F. Schaefer, *J. Am. Chem. Soc.* **117**, 446 (1995).
43. M. Schütz, T. Bürgi, S. Leutwyler, H. B. Bürgi, *J. Chem. Phys.* **99**, 5228 (1993); W. Klopper and M. Schütz, *Chem. Phys. Lett.* **237**, 536 (1995); T. Bürgi, S. Graf, S. Leutwyler, W. Klopper, *J. Chem. Phys.* **103**, 1077 (1995); W. Klopper, M. Schütz, H. P. Lüthi, S. Leutwyler, *ibid.*, p. 1085; J. G. C. M. van Duijneveldt–van de Rijdt and F. B. van Duijneveldt, *Chem. Phys. Lett.* **237**, 560 (1995); D. Sabo, Z. Bačić, T. Bürgi, S. Leutwyler, *ibid.* **244**, 283 (1995).
44. J. K. Gregory and D. C. Clary, *J. Chem. Phys.* **102**, 7817 (1995).
45. Mathematica 2.0, Wolfram Research, Champaign, IL; S. Wolfram, *Mathematica* (Addison-Wesley, Redwood City, CA, ed. 2, 1991).
46. I gratefully acknowledge the on-going contributions of R. S. Berry and J. P. K. Doye to this research and financial support from the Royal Society of London.

Water Clusters

K. Liu, J. D. Cruzan, R. J. Saykally

A surge of progress in both laser spectroscopy experiments and theoretical dynamics methods has facilitated new, highly detailed studies of water clusters. The geometrical structures and hydrogen-bond tunneling pathways of the water trimer, tetramer, pentamer, and hexamer systems have recently been characterized with global analysis of potential surfaces, diffusion Monte Carlo calculations, and far-infrared laser vibration-rotation tunneling spectroscopy. Results from these and other studies are yielding important insights into the cooperativity effects in hydrogen bonding, aqueous solvation, and hydrogen-bond network rearrangement dynamics, which promise to enhance our understanding of solid and liquid water behavior.

The study of van der Waals clusters is a very active subfield of cluster science (*1*, *2*). Arguably, the most important weakly bound complexes are pure water clusters. They have been directly implicated in several contemporary problems, including the formation of acid rain (*3*), the anomalous absorption of sunlight by clouds (*4*), and the nucleation of water droplets (*5*). Moreover, the use of water clusters in an indirect context offers an exciting prospect for important scientific advances in untangling the molecular details, for example, of aqueous solvation, cooperativity in hydrogen bonding, and hydrogen-bond network rearrangement dynamics that are so prevalent in the behavior of liquid water (*6*). The strong, directional intermolecular bonding and the capacity of water to act both as a double donor and a double acceptor of hydrogen bonds make water clusters less suitable for a rigorous theoretical treatment than other simple, weakly bound systems. Nevertheless, a recent surge of progress both in theory and experiment has made it possible to study water clusters at an unprecedented level of detail. In this article, we survey some of these developments and the chemical insight that has been gained from them.

Structures of Small Water Clusters

Theory and experiment are in fairly good agreement for the structure of the water dimer, determined spectroscopically in 1977 by Dyke, Mack, and Muenter (*7*). A number of recent high-level ab initio calculations (8) have predicted the structures of larger water clusters (Fig. 1). All the calculations predict that a quasi-planar cyclic form with each monomer acting as both a single donor and single acceptor, and with the free hydrogens oriented above and below the ring, constitutes the lowest energy structure for the trimer, tetramer, and pentamer. For the heptamer and larger clusters, a tendency toward three-dimensional (3D) structures is predicted, with the nature of the hexamer structure being ambiguous (*9*). In this evolution of structure with cluster size, the critical feature is the competition between maximizing the number of hydrogen bonds and minimizing the geometrical strain. The highest level ab initio calculations (*10*) predict a 3D cage structure to be the most stable for the hexamer, although at least three other structures lie within 0.3 kcal/mol and vibrational-averaging effects are likely to change their ordering. Interestingly, the predicted ring forms of the trimer, pentamer, and heptamer have no symmetry elements and are therefore chiral.

Our recent far-infrared laser vibration-rotation tunneling (VRT) spectroscopy experiments (*11*) support the theoretical predictions. For the trimer (*12*), tetramer (*13*), and pentamer (*14*), we found rotational energy level patterns that are rigorously those of a symmetric rotor ($A = B > C$, where A, B, and C are reciprocal moments of inertia, for example, $A = \hbar^2/2I_a$, where $\hbar$ is Planck's constant divided by 2π). In the case of the trimer, we could separately determine precise values for each of the three rotational constants and, therefore, definitively establish that the structure is an oblate symmetric rotor conforming rather closely to the predictions. Moreover, the large observed negative inertial defect ($I_c - I_b - I_a$) testifies to extensive out-of-plane motions by the free hydrogens. As discussed later, it is these large amplitude motions of the free hydrogens, actually a torsional motion of the water monomers about their donor hydrogen-bond axes ("flipping"), that produces the observed symmetric rotor spectrum through vibrational averaging over the totally asymmetric equilibrium structure.

For the tetramer and pentamer, we have not yet been able to extract such complete information. Precise values were deduced for the $A = B$ rotational constants, but the value for C (describing rotation about the symmetry axis) could only be estimated through simulations of the VRT intensity patterns. Nevertheless, the resulting precision was sufficient to unambiguously establish that the struc-

---

The authors are in the Department of Chemistry, University of California, Berkeley, CA 94720–1460, USA.

tures of the water clusters responsible for the observed spectra were indeed the quasi-planar rings predicted by theory (*8*). Furthermore, these spectra permitted estimates of the O–O distances to be extracted for each of the clusters, yielding a quantitative experimental measure of the hydrogen-bond cooperativity (Fig. 2). Very recently, we have also observed a VRT spectrum of the water hexamer (*15*). Although analysis has not yet been completed, the carrier of this spectrum appears most consistent with the predicted cage structure (*10*). On the basis of the above data, the overall agreement between ab initio theory and experiment with respect to the structures of small water clusters seems quite good. Measurements of trimer and tetramer VRT bands near 500 cm^{-1} by Fellers *et al.* (*16*) with tunable diode laser spectroscopy will soon provide additional comparisons.

Hydrogen-Bond Network Rearrangement Dynamics

The 6D intermolecular pair potential surface (IPS) of the water dimer contains a maximum of 16 identical "versions" of the global minimum structure, differing only by permutations of identical atoms that do not break chemical bonds. Actually, the number of versions is halved by the existence of a plane of symmetry in the dimer (*7*). Three low-energy pathways connecting the eight distinct versions have been identified through group theoretical analysis of the splitting patterns that accompany the rotational structure in a suitably high-resolution spectroscopy measurement, in conjunction with ab initio calculations (*17*). The dynamics that take place along these pathways occur by quantum tunneling through potential energy barriers and are termed "acceptor tunneling" (tantamount to a 180° rotation of the hydrogen-bond acceptor about its symmetry axis), "donor-acceptor interchange," and "donor" or "bifurcation" tunneling (interchange of the free and bonded hydrogens on the donor monomer). Each of these processes actually involves concerted motions of both monomers. The barrier heights for the three pathways have been calculated to be 206 cm^{-1}, 304 cm^{-1}, and 658 cm^{-1} kcal/mol (*18*).

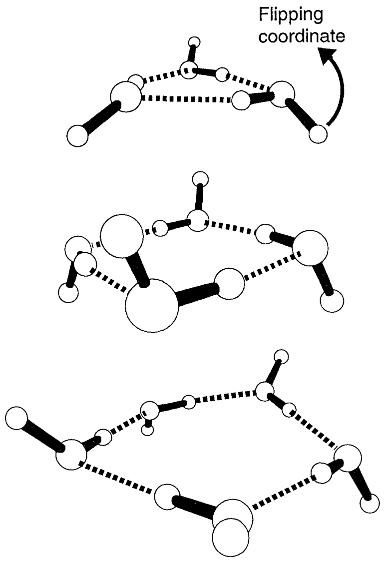

Fig. 1. Theoretically predicted equilibrium structures of the water trimer, tetramer, and pentamer (*8*), which have been confirmed by far-infrared VRT spectroscopy experiments. The dashed lines represent hydrogen bonds. The "flipping" motion (indicated by the arrow) of the free hydrogens causes averaging over the asymmetric equilibrium structures and produces the symmetric rotor behavior observed in the VRT spectra.

In general, a cluster of n water molecules will possess $6n - 6$ intermolecular degrees of freedom, and the corresponding IPS will exhibit a maximum of $2^n \times n! \times 2$ versions of the global minimum, which will be connected by a number of rearrangement pathways that do not involve the breaking of any chemical bonds. These paths can be systematically identified by the use of computer simulations with simple empirical potentials, subsequently refined by ab initio calculations and eigenvector-following methods, as demonstrated by Wales (*19*). Simple Hückel-type calculations can then yield approximate results for the effects of quantum tunneling on the energy level structures of the clusters (*19*), whereas emerging diffusion Monte Carlo methods can produce essentially exact results (for the nodeless states), limited only by the ability of the empirical potential to reproduce the true IPS (*20*). The combined force of these new theoretical approaches and VRT spectroscopy experiments makes it possible to extend the detailed knowledge developed for the water dimer dynamics to larger cluster systems.

The 12D trimer IPS exhibits 96 distinct versions of the global minimum energy structure. Two low-barrier hydrogen-bond network rearrangement (HBNR) pathways have been unambiguously identified (*12, 19*): the "flipping" motion of a single monomer and "bifurcation," essentially the same donor tunneling motion identified for the dimer, for which Fowler and Schaefer (*21*) have calculated barrier heights of 0.26 and 2.0 kcal/mol, respectively. A third pathway was postulated by Wales (*19*) to produce small splittings unobservable with the present VRT experiment. The flipping dynamics have been treated extensively by Leutwyler and collaborators, who used 1D, 2D, and 3D models to approximately describe the coupled torsional motions and associated potential surfaces (*22*); however, the agreement of these simplified models with experiment is not very satisfactory, most probably because of the neglect of other degrees of freedom.

The HBNR dynamics in the tetramer appear to be simpler. Although the 18D IPS exhibits a large number (768) of possible versions of the global minimum, its highly symmetric (S_4) structure, a ring analogous to cyclobutane (*8, 23*), greatly reduces this number and implies that the pathways for interconverting these versions involve both relatively concerted motions of the hydrogens and some heavy atom motion. This situation, combined with the generally higher potential energy barriers that result from cooperativity, implies a much longer time scale for the tunneling dynamics. The VRT experiments of Cruzan *et al.* (*13*) revealed a symmetrical doublet splitting in the eigenstates comparable in magnitude to the trimer quartet (donor tunneling) splittings. Recently, an additional small doubling of all lines in the $K = 2$ states was observed (K quantizes the angular momentum about the symmetry axis of the molecule) (*24*). Examination of the IPS by Schütz *et al.* (*23*) revealed no low-barrier paths for degenerate (between versions) rearrangements; instead, several different local minimum structures connected to the global minimum by low-energy, higher order stationary points were found. However, Wales (*25*) has identified a possible low-barrier degenerate rearrangement involving a "bifurcation plus single flip" on a single monomer. In any case, it will be interesting to explore in more detail the effects of these complicated nondegenerate rearrangements for the tetramer.

The pentamer is similar to the trimer, except that its chiral global minimum structure is a puckered ring, like cyclopentane (*8, 26*), which implies that both the flipping and donor tunneling pathways will involve heavy atom motion, leading to relatively quenched HBNR tunneling. In his exploration of the 24D IPS with its 7680 identical global minima, Wales (*26*) found that both of the above rearrangement paths have low barriers and should produce observable tunneling effects. He also identified 10 additional local minima in the IPS connected to the global minimum by 14 different tunneling pathways, and there are probably many more. Of these tunneling pathways, eight had barriers below 200 cm^{-1} and could therefore contribute to the HBNR dynamics in the low-lying energy levels of the pentamer. Interestingly, no tunneling splittings have yet been detected in the VRT spectra of $(D_2O)_5$ measured by Liu *et al.* (*14*). Diffusion Monte Carlo calculations by Gregory and Clary (*27*) predict a reduction in the donor tunneling of 67% and a reduction in the flipping splittings of 99.5% relative to $(D_2O)_3$. If these predictions are correct, then such tunneling effects should indeed be observable.

The VRT spectra of the H_2O hexamer measured by Liu *et al.* (*15*) exhibit a small triplet splitting with a characteristic intensity pattern. This splitting can be rationalized in terms of a single low-barrier degenerate rearrangement that involves the exchange of the hydrogen-bonded and free hydrogens on one monomer unit; two similar monomer units in a single donor–single acceptor bonding geometry are required to produce the observed triplet spectral pattern. However, the fact that at least 37 distinct local minima have been located on the 30D IPS (*9*) implies that nondegenerate tunneling processes are likely to contribute to the splitting as well.

The situation for larger water clusters promises to be quite interesting, as the role of nondegenerate tunneling processes involving numerous low-energy minima in the IPS becomes more pronounced in the HBNR dynamics. Nevertheless, some of the general features that have been characterized for the smaller clusters (such as flipping and bifurcation) may well contribute to the larger systems as well as to the dynamics of the liquid, because the associated barrier heights are comparable with or larger than kT at room temperature (where k is Boltzmann's constant and T is temperature).

Toward a Genuine Molecular Model of the Liquid

Many different models and approaches have been developed to calculate the unusual properties of condensed water in terms of the properties of its constituent molecules. Despite impressive advances, none has been entirely successful. Computer simulations using simple effective pair potentials have arguably provided the deepest insight into the molecular details of liquid properties and dynamics (*28*), and a large number of water pair potentials have appeared. The considerable success of this approach notwithstanding, none of these potentials can reproduce more than a few liquid (or solid) properties, even though the thermodynamic state of the system is held fixed in the simulations (*29*). This is mainly a consequence of the use of oversimplified potential energy functions. The most popular effective potentials are explicitly pairwise additive and include the crucial effects of cooperativity only implicitly, through the potential parameters. These, in turn, are obtained through fits to ab initio results and condensed phase measurements. Several recent efforts have produced nonadditive polarizable potentials (*30*), but although these are an improvement, they have not qualitatively changed the situation. Most effective potentials also assume rigid monomers, whereas the water molecule is itself actually somewhat flexible and distortable. Effective potentials based on flexible monomers have also appeared recently, but they have so far been based entirely on ab initio calculations (*31*). Parrinello and co-workers (*32*) have used their powerful ab initio molecular dynamics approach to investigate liquid water, elegantly addressing these problems but nevertheless relying exclusively on an ab initio potential.

An attractive alternative is to use a "genuine" molecular potential energy model in simulations of condensed water. By "genuine," we mean with explicit parameterization and functionality for the proper description of pairwise, three-body, four-body, and many-body interactions among flexible monomers. Clementi and co-workers (*33*) have attempted to develop such potentials from ab initio calculations on the water dimer, trimer, and larger clusters, as have others (*34*). However, the difficulty in calculating molecular interactions with sufficient accuracy for this purpose is well documented (*2*). It seems advisable to find an experimental route to the determination of an accurate water pair potential, as well as to the three- and higher-body effects, at least to calibrate and complement the ab initio results.

The obvious starting point for developing a genuine molecular model for liquid water is to obtain an accurate and detailed IPS, which will rigorously describe the interactions between two water molecules at all distances and orientations. If the water molecules are frozen at their intramolecular vibrationally averaged ground-state structures, the dimer IPS will involve six intermolecular coordinates. The most direct route to this explicit pair potential is through precise measurement of the intermolecular vibrations and geometric structure of the water dimer (*11*). Previous spectroscopic investigations of the dimer have been reviewed by Fraser (*35*). Pugliano and Saykally (*36*) recently used tunable far-infrared lasers to make the first definitive measurement of dimer intermolecular vibrations, which are accompanied by intricate rotational and hydrogen-bond tunneling effects. Continued refinement of the technology has now permitted us to measure VRT spectra of nearly all the fundamental intermolecular vibrations of both $(H_2O)_2$ and $(D_2O)_2$. We are in the process of inverting these data to extract the dimer IPS, using the Wigner discrete variable rep-

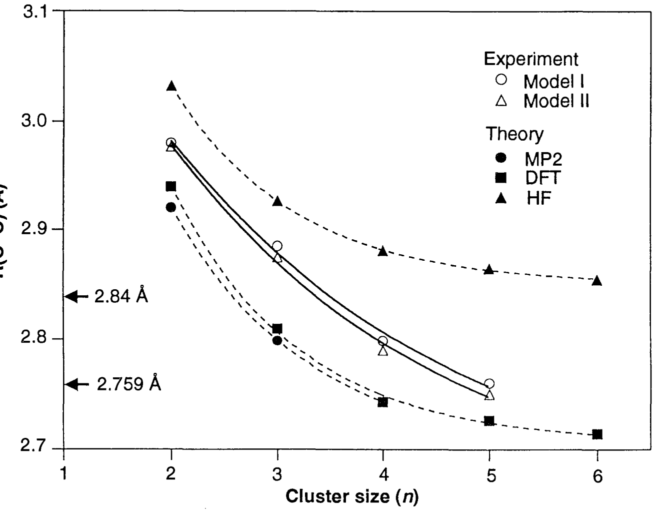

Fig. 2. The O–O distance [R(O–O)] versus cluster size, obtained from VRT spectroscopy studies of water clusters. Also plotted are the corresponding separations obtained at three different levels of theory (*18*): Hartree-Fock (HF), Møller-Plesset second-order perturbation theory (MP2), and density functional theory (DFT). The experimental O–O distances in liquid water (2.84 Å at 4°C) (*50*) and Ih ice (2.759 Å at 223 K) (*51*) are indicated by the arrows. Two methods of extracting R(O–O) from the measured rotational constants were used. Manifesting the hydrogen-bond cooperativity, both methods produced an exponential O–O distance contraction with increasing cluster size. In model I (*23*), the averaged center-of-mass (COM) separations were obtained by adjusting the uniquely determinable separations between the monomers (treating each monomer as a point mass) in a unique averaged geometry, a pseudo-diatomic for the dimer or an equilateral planar polygon for the ring complex (a nonequilateral or puckered polygon does not represent the average symmetric rotor), to reproduce the only reliable experimental structure observable—averaged B for the dimer or $A = B$ for the ring clusters. The COM trend thus obtained is subsequently scaled (multiplied by 0.977) to the previously determined dimer R(O–O), 2.98 Å (*15*), to produce the O–O separations. Fitting the R(O–O) values for $(D_2O)_n$ (n = 2, 3, 4, and 5) resulted in the following expression: $R^{(n)}$ (O–O) = 2.639 + 0.6981 × exp($-0.3566n$). In model II (*22*), the R(O–O) values of the trimer, tetramer, and pentamer were obtained by assuming the ab initio equilibrium geometric details and varying the distance of the monomers from the cluster COM (while fixing the other coordinates) until agreement with the measured moments of inertia was reached: Note that the ab initio structures are only slightly asymmetric for the equilibrium trimer and pentamer. Similar R(O–O) fitting yielded $R^{(n)}$(O–O) = 2.642 + 0.7266 × exp($-0.3868n$).

resentation approach of Leforestier (*37*) to describe the coupled 6D dynamics.

The nonpairwise interactions, or cooperativity, among hydrogen-bonded water molecules have a number of well-known manifestations, including an increased hydrogen-bond strength, elongation of the donor O–H bond, a red shift in the donor asymmetric stretching vibration, shortening of the O–O distance, and an increase of the monomer dipole moment from its gas phase value of 1.8 D to a value of ~2.6 D in the liquid (*8*). These effects can be quantified through precise spectroscopic investigations of small water clusters. The first such result is shown in Fig. 2, in terms of the O–O distance contraction. Calculations indicate that the principal source of nonadditivity in water hydrogen bonding is many-body induction (*38*). Dispersion effects are considerably smaller, whereas effects of many-body exchange and charge transfer are still being debated (*39*). The importance of exchange quadrupole interactions in rare gas–containing trimers was revealed by the VRT experiments of Elrod and Saykally (*38*), and these may be significant for aqueous systems as well.

A goal of water cluster research is to produce an effective potential suitable for use in condensed matter simulations. With the VRT data obtained so far, we can begin to assess and refine the existing potentials. The new dynamics methods are of crucial importance for this purpose, as they permit a direct (albeit limited) comparison of experiment and theory. Althorpe and Clary (*40*) have used an approximate method to examine several of the most popular water effective pair potentials with respect to their ability to reproduce the HBNR tunneling splittings in the dimer, and Gregory and Clary (*20, 27, 41*) have extended this work to higher clusters with the use of exact diffusion Monte Carlo methods. From their work, it is clear that the simple effective pair potentials used for liquid simulations are not capable of describing the gas phase water clusters (they were not designed to). However, a reparameterized version of Stone's anisotropic site potential (ASP) (*42*), which includes an iterated many-body induction term and many-body dispersion, seems to do quite well in accounting for most experimentally observed features of the trimer, tetramer, and pentamer spectra. Hence, we may now be poised to generate significantly improved effective potentials that can describe the liquid and solid phases of water better than their predecessors.

Aqueous Solvation

One of the most often stated goals of cluster research is to elucidate the molecular details of solvation phenomena, and nowhere is this more important than in the case of water. Indeed, some important insights into the molecular nature of aqueous solvation have recently been obtained through studies of water clusters. Castleman and coworkers (*43*) found a striking similarity between gaseous hydrated proton clusters and the icosahedral clathrate structures formed when hydrophobic solutes are dissolved in water and frozen. They showed that a closed hollow structure formed by 20 hydrogen-bonded water molecules arranged into 12 concatenated pentagons (considering only oxygen atoms) with 10 free exterior hydrogens encapsulates both H^+ and H_3O^+ ions, thereby explaining the occurrence of "magic numbers" (numbers indicative of particularly stable structures) in the mass spectra of water clusters. Similar truncated icosahedral structures of hydrogen-bonded water molecules consisting of 12 pentagons plus some number of hexagons (similar to the fullerenes) form the closed clathrate cages that enclose the hydrophobe. Pentagons generally dominate over hexagons by about 8:1 in clathrates (*43*), and it is the pentagon that provides the ability to form closed surfaces. The cyclic water pentamer and hexamer described earlier are very similar to the basic structural units for these clathrates.

The cyclic water pentamer appears to be a similarly fundamental structure in the hydration of biomolecules. For example, x-ray studies revealed that the protein crambin has hydrophobic clefts wherein 16 waters of hydration are arranged into a cap of concatenated pentagons surrounding a leucine methyl group (*44*). Similar behavior has also been found in other proteins (*45*) and in DNA polymers (*46*). Computer simulations indicate that pentagons are the dominant water structures in hydrophobic hydration (*46*), but also that there is an increasing tendency to form six- and seven-membered rings as the hydrophilicity of the solute increases. The crucial role of pentagons in hydrophobic hydration is again that of providing the curvature required for water to order itself around the surface of the hydrophobe. This provides a structural explanation for why the entropy change dominating the hydrophobic effect is proportional to the surface area of the solute (*48*). Water apparently seeks to enclose a hydrophobe with a polyhedral structure as a means of minimizing disruption of the preferred tetrahedral hydrogen-bond network.

Another probe of aqueous solvation phenomena through the study of water clusters was recently demonstrated by Zweir and co-workers (*49*). Using their resonant ion dip infrared spectroscopy method, they have recorded low-resolution infrared spectra of benzene-$(H_2O)_n$ clusters with $n = 1$ to 7 in the C–H and O–H stretch regions. The frequency shifts and intensities of the O–H absorptions probe cooperative effects in the hydrogen bonding in the $(H_2O)_n$ cluster. By comparison with computed infrared spectra and with the earlier infrared predissociation work of Lee and co-workers (*50*) and similar results by Huisken *et al.* (*51*), these researchers concluded that the water trimer, tetramer, and pentamer within the benzene $(H_2O)_n$ clusters have the same types of ring structures as do the pure water clusters. Furthermore, their results show that the hexamer and heptamer adopt noncyclic geometries in the benzene complexes, with several water molecules acting as double donors to other waters. These are precisely the cluster sizes for which noncyclic structures of pure water clusters are predicted by theory (*10*) to become lower in energy than the quasi-planar cyclic forms, which is in accord with our VRT spectroscopy results for the hexamer (*15*). In general, these results support the notion that water seems to retain much of its intrinsic structure in the presence of solute molecules.

Future Considerations

Given the high (80:1) signal-to-noise ratio achieved in the current far-infrared VRT experiments for the water hexamer (*15*), extensions of these measurements to higher clusters are inevitable. The newly developed infrared cavity ringdown laser absorption spectroscopy method (*52*) is likely to become a useful tool for studying mid-infrared spectra of water clusters as well (the water pentamer has already been measured by this method). The combination of these and other new laser spectroscopy experiments with the global analysis of potential surfaces and diffusion Monte Carlo methods described in this article are likely to generate a wealth of information regarding the intricate details of how water molecules interact. This should serve as a useful complement to the results emerging from quantum chemistry and ab initio molecular dynamics in the quest for a quantitative description of the condensed phases of water.

REFERENCES AND NOTES

1. Special issue on *Structure and Dynamics of van der Waals Clusters*, B. J. Howard, Ed., *Faraday Discuss.* **97** (1994).
2. Special issue on van der Waals Clusters II, J. Michl, Ed., *Chem. Rev.* **94**, 7 (1994).
3. C. E. Kolb *et al.*, *J. Am. Chem. Soc.* **116**, 10314 (1994); K. Morokuma and C. Muguruma, *ibid.*, p. 10316.
4. H. R. Carlon, *Infrared Phys.* **19**, 549 (1979).
5. ______, *J. Phys. D* **17**, 1221 (1984).
6. I. Ohmine, *J. Phys. Chem.* **99**, 6767 (1995).
7. T. R. Dyke, *J. Chem. Phys.* **66**, 492 (1977); ______, K. M. Mack, J. S. Muenter, *ibid.*, p. 498.
8. S. S. Xantheas and T. H. Dunning, *ibid.* **99**, 8774 (1993) and references therein; J. van Duijneveldt-van de Rijdt and F. B. van Duijneveldt, *Chem. Phys.* **175**, 271 (1993); R. Knochenmuss and S. Leutwyler, *J. Chem. Phys.* **96**, 5233 (1992).

9. C. J. Tsai and K. D. Jordan, *Chem. Phys. Lett.* **213**, 181 (1993).
10. K. Kim, K. D. Jordan, T. S. Zwier, *J. Am. Chem. Soc.* **116**, 11568 (1994).
11. R. J. Saykally and G. A. Blake, *Science* **259**, 1570 (1993).
12. N. Pugliano and R. J. Saykally, *ibid.* **257**, 1937 (1992); K. Liu *et al.*, *J. Am. Chem. Soc.* **116**, 3507 (1994); K. Liu *et al.*, *Faraday Discuss.* **97**, 35 (1994).
13. J. D. Cruzan *et al.*, *Science* **271**, 59 (1996).
14. K. Liu, M. G. Brown, J. D. Cruzan, R. J. Saykally, *Science* **271**, 62 (1996).
15. K. Liu *et al.*, in preparation.
16. R. Fellers *et al.*, in preparation.
17. L. H. Coudert and J. T. Hougen, *J. Mol. Spectrosc.* **139**, 259 (1990).
18. B. J. Smith *et al.*, *J. Chem. Phys.* **92**, 1240 (1990).
19. D. J. Wales, *J. Am. Chem. Soc.* **115**, 11180 (1993).
20. J. N. Gregory and D. C. Clary, *J. Chem. Phys.* **102**, 7817 (1995); *Chem. Phys. Lett.* **228**, 547 (1994).
21. J. E. Fowler and H. F. Schaefer, *J. Am. Chem. Soc.* **117**, 446 (1995).
22. D. Sabo, Z. Bacic, T. Bürgi, S. Leutwyler, *Chem. Phys. Lett.* **244**, 283 (1995); T. Bürgi, S. Graf, S. Leutwyler, W. Klopper, *J. Chem. Phys.* **103**, 1077 (1995); W. Klopper, M. Schütz, H.-P. Lüthi, S. Leutwyler, *ibid.*, p. 1085; W. Klopper and M. Schütz, *Chem. Phys. Lett.* **237**, 536 (1995); M. Schütz, T. Bürgi, S. Leutwyler, H. B. Bürgi, *J. Chem. Phys.* **99**, 5228 (1993); *ibid.* **100**, 1780 (1994).
23. M. Schütz, W. Klopper, H.-P. Lüthi, S. Leutwyler, *J. Chem. Phys.* **103**, 6114 (1995).
24. J. D. Cruzan *et al.*, in preparation.
25. D. J. Wales, unpublished results.
26. D. J. Wales *et al.*, *J. Am. Chem. Soc.*, in preparation.
27. J. N. Gregory and D. C. Clary, unpublished results.
28. F. H. Stillinger, *Science* **209**, 451 (1980); A. C. Belch and S. A. Rice, *J. Chem. Phys.* **86**, 5676 (1987); R. J. Speedy and M. Mezei, *J. Phys. Chem.* **89**, 171 (1985).
29. W. L. Jorgensen, J. Chandrasekhar, J. D. Madura, R. W. Impey, M. L. Klein, *J. Chem. Phys.* **79**, 926 (1983); M. Townsend, S. A. Rice, M. D. Morse, *ibid.*, p. 2496.
30. K. Watanabe and M. L. Klein, *Chem. Phys.* **131**, 157 (1989); P. Cieplak, P. Kollman, T. Lybrand, *J. Chem. Phys.* **92**, 6755 (1990).
31. G. Corongiu, *Int. J. Quantum. Chem.* **42**, 1185 (1992).
32. K. Laasonen, M. Sprik, M. Parrinello, R. Car, *J. Chem. Phys.* **99**, 9081 (1993).
33. G. Corongui and E. Clementi, *Chem. Phys. Lett.* **214**, 367 (1993).
34. P.-O. Astrand, A. Wallqvist, G. Karlstrom, *J. Chem. Phys.* **100**, 1262 (1994).
35. G. Fraser, *Int. Rev. Phys. Chem.* **10**, 189 (1991).
36. N. Pugliano and R. J. Saykally, *J. Chem. Phys.* **96**, 1832 (1992); N. Pugliano *et al.*, *ibid.* **98**, 6617 (1993).
37. C. Leforestier, *ibid.* **101**, 7360 (1994).
38. M. J. Elrod and R. J. Saykally, *Chem. Rev.* **94** (7) 1975 (1994).
39. B. F. King and F. Weinhold, *J. Chem. Phys.* **103**, 333 (1995).
40. S. C. Althorpe and D. C. Clary, *ibid.* **101**, 3603 (1994).
41. J. N. Gregory and D. C. Clary, *ibid.*, in preparation.
42. C. Millot and A. J. Stone, *Mol. Phys.* **77**, 439 (1992).
43. P. M. Holland and A. W. Castleman Jr., *J. Chem. Phys.* **72**, 5984 (1980); S. Wei, Z. Shi, A. W. Castleman Jr., *ibid.* **94**, 3268 (1991); X. Yang and A. W. Castleman Jr., *J. Am. Chem. Soc.* **111**, 6845 (1989).
44. M. M. Teeter, *Proc. Natl. Acad. Sci. U.S.A.* **81**, 6014 (1984).
45. T. Baker, E. Dodson, G. Dodson, D. Hodgkin, R. Hubbard, in *Crystallography in Molecular Biology*, D. Moras, J. Drenth, B. Strandberg, D. Suc, K. Wilson, Eds. (Plenum, New York, 1985), pp. 179–192.
46. S. Neidle, H. Berman, H. S. Shieh, *Nature* **288**, 129 (1980).
47. T. K. Kim and M. S. Jhon, *J. Mol. Liq.* **59**, 179 (1994).
48. T. Head-Gordon, *Proc. Natl. Acad. Sci. U.S.A.* **92**, 8308 (1995).
49. R. N. Pribble and T. S. Zwier, *Science* **265**, 75 (1994).
50. M. F. Vernon *et al.*, *J. Chem. Phys.* **77**, 47 (1982); R. H. Page, J. G. Frey, Y.-R. Shen, Y. T. Lee, *Chem. Phys. Lett.* **106**, 373 (1984).
51. F. Huisken, M. Kaloudis, A. Kulcke, D. Voelkel, *Infrared Phys. Technol.* **36**, 171 (1995).
52. J. J. Scherer *et al.*, *Chem. Phys. Lett.* **245**, 273 (1995).
53. R.J.S. thanks A. D. Buckingham, D. Wales, and D. Clary for their hospitality during the writing of this review and the Churchill College of Cambridge University for a fellowship. The Berkeley work is supported by the NSF (grant #CHE-9424482).

Semiconductor Clusters, Nanocrystals, and Quantum Dots

A. P. Alivisatos

Current research into semiconductor clusters is focused on the properties of quantum dots—fragments of semiconductor consisting of hundreds to many thousands of atoms—with the bulk bonding geometry and with surface states eliminated by enclosure in a material that has a larger band gap. Quantum dots exhibit strongly size-dependent optical and electrical properties. The ability to join the dots into complex assemblies creates many opportunities for scientific discovery.

Cluster science is devoted to understanding the changes in fundamental properties of materials as a function of the size, evolving from isolated atoms or small molecules to a bulk phase. In the case of semiconductors, this evolution is remarkable (*1*). For example, the band gap in CdS can be tuned between 4.5 and 2.5 eV as the size is varied from the molecular regime to the macroscopic crystal, and the radiative lifetime for the lowest allowed optical excitation ranges from tens of picoseconds to several nanoseconds (*2*). The energy above the band gap required to add an excess charge decreases by 0.5 eV (*3*). The melting temperature increases from 400° to 1600°C (*4*), and the pressure required to induce transformation from a four- to a six-coordinate phase decreases from 9 to 2 GPa (*5*). This enormous range of fundamental properties is realized in a material of a single chemical composition, purely by increasing the size, and can be used to advantage in light-emitting diodes (*6, 7*) and other optical and electrical devices in the future. Two peculiar characteristics of semiconductors influence the ways in which we think of an ideal semiconductor cluster, which is often called a quantum dot.

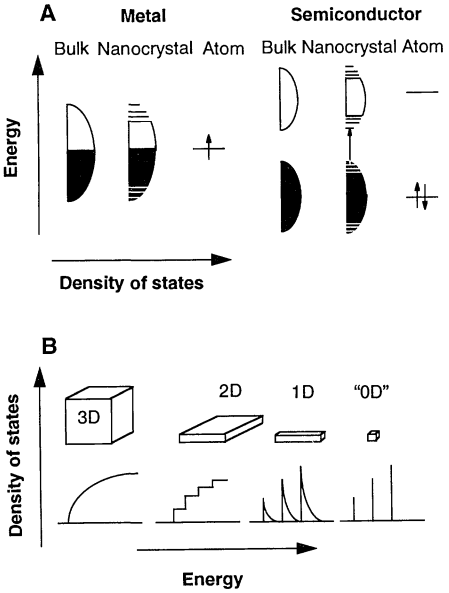

Fig. 1. (**A**) Schematic illustration of the density of states in metal and semiconductor clusters. (**B**) Density of states in one band of a semiconductor as a function of dimension.

First, it is important to realize that in any material, substantial variation of fundamental electrical and optical properties with reduced size will be observed when the electronic energy level spacing exceeds the temperature. In semiconductors, this transition occurs for a given temperature at a relatively large size compared to metals, insulators, or molecular crystals. This difference can be understood by considering that the bands of a solid are centered about atomic energy levels, with the width of the band related to the strength of the nearest-neighbor interactions. In the case of van der Waals or molecular crystals, the nearest-neighbor interactions are weak, the bands in the solid are very narrow, and consequently, not much size variation in optical or electrical properties is expected or observed in the nanocrystal regime. As cluster size increases, the center of a band develops first and the edges last. Thus, in metals, where the Fermi level lies in the center of a band, the relevant energy level spacing is

---

The author is in the Department of Chemistry, University of California, and Materials Sciences Division, Lawrence Berkeley Laboratory, Berkeley, CA 94720, USA.